Periodico di Mineralogia (2015), 84, 2, 323-339 DOI: 10.2451/2015PM0016

PERIODICO di MINERALOGIA
established in 1930

An International Journal of
MINERALOGY, CRYSTALLOGRAPHY, GEOCHEMISTRY,
ORE DEPOSITS, PETROLOGY, VOLCANOLOGY
and applied topics on Environment, Archaeometry and Cultural Heritage

Chemical and isotopic characterization of products of small-scale hypervelocity impacts: the Gebel Kamil event

Gian Paolo Sighinolfi[1], Gabriele Contini[1], Maurizio Barbieri[2,*] and Angela Nigro[2]

[1] Dipartimento di Scienze Chimiche e Geologiche, Università di Modena e Reggio Emilia
Via Giuseppe Campi 183, 41125 Modena
[2] Dipartimento di Scienze della Terra, Università degli Studi di Roma La Sapienza,
Piazzale Aldo Moro 5, 00185 Roma
[*] Correspondig author: *maurizio.barbieri@uniroma1.it*

Abstract

This study presents chemical and oxygen isotope data on a series of materials found in the area of the Gebel Kamil crater, a recent well preserved impact crater in southern Egypt, which was formed by the explosive impact of a metal projectile. Intracrateric target rocks, fallback deposits, impact vitreous ejecta (impactite) and recent or present-day aeolian sands have been analysed. Exposed crater wall rocks essentially consist of quartz arenites with minor siltstone beds chemically and isotopically quite distinct, the latter resulting enriched in lithophile elements (Al, K, Ba, Y, REE, etc.) and ^{18}O. Abundance of siderophile elements (Ni, Co, Cu) indicates that none of the exposed target rocks and recent aeolian sand deposits was contaminated by materials of the metal impactor. On the other hand, a projectile-derived component was found in all samples of fallback deposits and in impact melt ejecta. Lithophile element and isotope chemistry of the fallback deposit results intermediate between that of quartz arenite and silstone target rocks. White- light-coloured glassy ejecta representing a minor (< 10% vol.) component of the impact melted products are chemically and isotopically distinct from dark-coloured vitreous clasts. The latter are enriched in lithophile elements and also ^{18}O with respect to estimated "average" composition of the intracrateric target rocks. The presence of a projectile component in all samples of vitreous ejecta clasts suggests that melting of terrestrial material becomes extensive only when the projectile is directly involved in melting. The extreme variability of siderophile element ratios (e.g. Ni/Co, Ni/Cu) in materials (i.e., fallback deposits and vitreous ejecta) contaminated by projectile components suggests that significant element fractionation occurs during the explosive disruption of an impactor. A distinctive chemical and isotope signature of most of the impact melted products (i.e., dark vitreous ejecta), with respect to "average" composition of the exposed crater

target rocks, poses problems concerning the actual terrestrial material source. On the basis of knowledge of surface geological stratigraphy, we hypothesize that the terrestrial source material for most of impact melted products (i.e., the dark impactites), is represented by a 2 m tick weathered unconsolidated cover enriched in lithophile elements originally present on the preimpact surface. The data suggest that in the case of small-scale explosive impacts effective melting of terrestrial material occur only at or nearly the earth's surface with the direct involvement of the projectile.

Key words: Impact crater; Chemical data; ^{18}O data.

Introduction

The Gebel Kamil crater is a very recent and well preserved impact crater in south-eastern Egypt. It was formed by an explosive hypervelocity impact of a metallic impactor on hypersilicic sedimentary formations. Owing to the freshness and perfect exposure of the target crater rocks and of the pristine localization of all ejected impact products (terrestrial ejecta, fragments of the projectile and vitreous clasts), geochemical and isotope investigations on these materials may contribute to the knowledge of the global effects of a hypervelocity impact of a metallic body on silicate terrains. In particular, comparative studies on substratum target rocks and products of impact thermal metamorphism (vitreous ejecta) may provide detailed information on the source material for individual impact products, i.e. which terrestrial target material was effectively involved in impact melting. In addition, taking into account the contrasting nature of the Gebel Kamil impactor (Ni-rich iron) and of the Kamil substratum rocks and surface formations (hypersilicic sediments and soils), analyses of siderophile elements in these formations may yield a better knowledge of areal dispersion patterns of projectile-derived components. Theoretically, this could represent an additional diagnostic parameter for the detection of impact explosive events, especially where primary structures were completely obliterated by surface alteration processes. Finally, analyses of the relative abundance of elements of almost exclusive extraterrestrial origin (i.e., Ni, Co, Cu, etc.) in materials contaminated by projectile components may be useful for testing possible element fractionation processes as a consequence of the explosive disruption, melting and volatilization processes of the impactor. To tackle some of these issues, the results of chemical and isotopic characterization of different materials present in the Gebel Kamil impact area are reported in this study. They include intracraterial target rocks and products of their disaggregation during impact (fallback deposits), products of impact thermal metamorphism (vitreous impactite ejecta) and surface sedimentary formations (recent or present day aeolian sands) surrounding the crater.

General features of the Gebel Kamil crater

The Gebel Kamil crater is a small (45 m diameter) and very well preserved impact crater in the south-eastern Egyptian Sahara (22°01'06"N, 26°05'15"E) excavated in hypersilicic sedimentary terrains belonging to the Gilf Kebir Formation, a Late Jurassic to Early Cretaceous formation predominantly made up of layered quartz arenites (Klitsch et al., 1979). After the first announcement of this discovery (Folco et al., 2010), a series of geological and geophysical investigations were carried out (Folco et al., 2011; Urbini et al.,

2012), which allowed the characterization of the crater structure, the distribution of terrestrial and projectile-derived ejecta around the crater, and the direction of incidence and impact angle of the metallic impact to be determined. No evidence of significant erosional features was observed in the crater and crater rim; therefore the material contained must have maintained its pristine localization. The very recent age of the Kamil event is confirmed by Sighinolfi et al., 2015 which indicates a most probable age between 1600-400 yrs BCE. Petrographic observations of the substratum rocks exposed on the internal crater walls (Urbini et al., 2012; Fazio et al., 2014) show that layered, pale-reddish, coarse quartz arenite made up of detrital quartz grains represents the most common rock type. Minor layers of fine-grained, very compact siliceous rocks (siltstones)) are interbedded with coarse-grain arenites; they increase toward the top of the sedimentary sequence. Petrological observations indicate that siltstones underwent strong lithification processes causing partial dissolution of the primary quartz grains followed by precipitation of silica cement. A kaolinite matrix is also present in such fine-grained rocks. Rocks from the crater walls, unlike those present as ejecta debris or associated to vitreous ejecta (lapilli and bombs), apparently don't show evidence of shock macro deformation textures (shatter cones). On the other hand, all exposed target rocks are characterized by the ubiquitarious presence of impact high density phases such as coesite (Sighinolfi et al., 2014). The bottom of the crater is filled with breccia lenses which to the NW are superimposed by well distinguishable fine-grained, whitish, finely-laminated deposits more than 1.60 m thick. These deposits consist of fallback material, namely sediments of powdered target rocks which were deposited in situ immediately after the impact. They contain wall rock fragments and impact products in the form of silicate and metal melt glass microparticles. Recent or present-day aeolian sands cover part of the northern crater wall and the crater floor. On the basis of the morphology and size of the Kamil crater, Urbini et al. (2012) calculated that the excavated volume (i.e., the volume of the crater between the top of the breccia lenses and the pre-impact surface) is approximately 3800 m^3. It should be considered that this volume is only in part represented by the exposed intracrateric compact target rocks (arenites and siltstones). In fact, the reconstruction of the pre-impact stratigraphic sequence based on seismic profiles (Urbini et al., 2012) indicates the presence on the preimpact surface of an approximately 2 m thick unconsolidated cover at the impact site. There isn't information about the composition of such unconsolidated cover. It could be constituted by alloctonous materials (i.e. aeolian sands) but more probably, it consists of in situ alteration products of substrate rocks. Most of the excavated materials are now present as a continuous veneer of ejecta, consisting of a chaotic mixture of boulders, blocks and fine-grained debris, extending in different directions up to a distance of about 500 m from the crater. Ejecta are essentially made up of terrestrial rocks (sandstones) characterized by a series of macro- and micro shock metamorphic features associated in some cases to impact melting (Fazio et al., 2014). In particular the presence of glass films coating shatter cone structures suggests that melting conditions could be at least in part achieved by frictional melting. Minor constituents of bulk-ejected material consist of a variety of partially or almost totally vitreous clasts (impactite) of variable mass (from tenths to few hundredths g), concentrated along the external border of the crater but also present inside the crater and in the less proximal ejecta blanket. Field observations indicate a progressive reduction of the mass of the impactite clasts with distance from the impact site. Macroscopically, the impactite clasts are quite variable in aspect, in terms of colour (from

light to dark grey) and density (from pumiceous to high-density clasts). By far the most abundant vitreous impactite clast ejecta consist of dark-coloured debris, ranging in colour from light grey to dark grey and black. Minor amounts of light-coloured impactite clasts of appreciable mass occur exclusively in the proximity of the crater. Usually, they are partially covered by a black patina and contain segregates and veinlets of black materials. X-ray analyses indicated that most black patina and segregates consist of amorphous material, possibly representing the product of terrestrial iron oxides segregated during impact. Light-coloured impactite clasts seem to have undergone rather variable shock melting (from moderate melting to almost total melting). Observations under the optical microscope normally reveal the presence of opaque spherules, probably representative of melting products of the metal projectile. In analogy with light-coloured clasts, also larger mass (> 100 g) dark impactite clasts occur exclusively within a relatively short distance (< 50 m) from the crater. Similarly to the light-coloured clasts, dark-coloured ejecta are characterized by a rather variable melting rate. Under the microscope they are enriched in opaque spherules, interpretable, according to Folco et al. (2011), as melted Fe-Ni droplets representing impactor-derived components together with Fe-Ni-rich silica glass. Investigations (Folco et al., 2012) carried out on the magnetic extract from soils as far as 1.3 km from the crater rim revealed the presence of microshrapnel of the projectile and of Fe-Ni-rich vesicular impact glass particles. The concentrations of Ni in these materials (Folco et al., 2013) suggest that the impact plume carrying impactor debris was somewhat wind-blown. Several lines of evidence (i.e., catastrophic disruption of the impactor into thousands of fragments, distribution of ejecta and morphology of the crater) document that the Kamil crater was produced by a hypervelocity impact rather than a low-velocity penetration crater. Assuming an impact angle of 45° as calculated by Urbini et al. (2012) and on the basis of the planar impact approximation of Melosh (2013) the maximum shock pressures at Kamil must have been comprised between 30GPa (5.0 k s-1 impact velocity) and 60 GPa (7.5 k s-1).

Analyzed parameters, materials and methods

Chemical and isotope parameters

The data reported in the present study refer to a group of chemical parameters which appear particularly suitable to investigate the arguments and problems cited in the previous paragraph. They include a group of main and trace lithophile elements (Al, K, Th, REE, Cr, Ba, Sr, V, Rb, Y, Ga) and Mo which allow a good chemical characterization of the different terrestrial formations present in the impact site, including compact substratum rocks and their impact products. The study reports also the data for some siderophile elements (Ni, Co and Cu) whose overabundances in the metallic impactor are in sharp contrast with their very low contents in the hypersilicic rocks and sediments of the Kamil area. So, their presence both in terrestrial formations and in impact products (vitreous ejecta) allows assessments of contamination rates from impactor-derived components. Data on chemical elements of questionable origin (terrestrial vs. meteoritic), such as iron, are omitted because they are not useful for the discussion. Oxygen isotope analysis ($^{18}O/^{16}O$) was carried out on a series of selected samples of all materials considered in this study (target rocks fallback sediments, vitreous ejecta and aeolian sands).

Analyzed materials and their localization

Information on the exact localization and some macroscopic features of part of the materials (target rock, fallback deposits, impactite ejecta and aeolian sands) considered in the present

study are given elsewhere (Sighinolfi et al., 2014). Here follows a list of samples submitted to chemical analysis and some additional data regarding their localization and macroscopic features:

1) Intracrateric target rocks (5 samples labelled TR) collected on the SSW wall of the crater. Sample TR-1, TR-2 and TR-3 are pale, pink quartz arenites. Sample TR-4 and TR-5 are white-grey siltstones collected on the SSW upper internal wall of the crater.

2) Intracrateric fallback deposit (6 samples labelled FB) was collected at the base of the crater. This deposit was sampled at different depths (from surface to 120 cm) with the use of a 30 mm diameter steel sampler (for collecting depths see Sighinolfi et al., 2014).

3) Vitreous ejecta clasts (9 samples labelled IC). The data refer to 7 individual white- or light-coloured vitreous clasts (sample IC-1, 2, 3, 4, 6, 7, 8) with mass varying from 16.2 to 103.1 g. They were all collected at relatively short distances (< 30 m) from the external crater rim. As regards the analysis of dark-coloured vitreous clasts, by considering their high abundance with respect to white-coloured vitreous clasts, some cumulative samples were prepared in loco by combining small fragments separated by individual clasts. This procedure would allow a reasonable assessment of the average composition of the entire mass of dark vitreous products. Two cumulative samples were prepared: one (sample IC 9) combining materials from 20 small (< 20 g) clasts collected at distances of over 30 m from the crater; the other (sample IC 10) from 4 larger dark clasts (> 30 g) collected in areas more proximal (< 30 m distant) to the crater.

Oxygen isotope analysis was carried out on some selected samples of the different materials of Gebel Kamil. They include crateric target rocks (samples TR-1, TR-2 TR-3 and TR-4), fallback deposits (samples FB-1, FB-2, FB-4 and FB-5), aeolian sands (samples SB-1 and SB-3) and ejected vitreous clasts (sample IC-1, IC-3, IC-5, IC-9 and IC-10). In addition, oxygen isotope analysis was also carried out on detrital quartz grains separated under the microscope from the IC-1 vitreous ejecta clasts (sample IQz-1).

Methods

Chemical analysis. Main and trace elements were determined by Plasma Mass Spectroscopy by using a Thermo Scientific XSERIES 2. Samples were crushed and pulverized in an agate mortar. 100-200 mg of the pulverized material was submitted to acid decomposition using the classical procedures (HCl-HF followed by HNO_3-HF attacks and dissolution of the residue in 2% HNO_3). Analytical errors should be estimated at less than 4% for main and trace constituents and 5% for U and Th.

Stable isotope analysis. Detailed information on the analytical method used was reported elsewhere (see e.g. Longinelli et al., 2011). About 6 mg of finely ground material was made to react with BrF_5 in vacuo for at least 12 h. The O_2 obtained from the reaction was converted to CO_2 by cycling over hot graphite in the presence of a platinum catalyst and then measured on a Finnigan Delta S mass spectrometer.

Analytical results

Chemical data

Analytical results for some major and trace lithophile and siderophile constituents are presented in Table 1. REE data are reported in graphic form in Figures 1-4. Figure 1 reports REE patterns in intracraterial sandstone and siltstone target rocks, Figure 2 in fallback deposits, Figure 3 in light- and dark-coloured impactite ejecta and Figure 4 in aeolian sands, all normalized respect to Chondrite (McDonough and Sun, 1995; Melosh, 2013). The low contents of main rock constituents (i.e., Al and K) in both quartz arenite and siltstone target rocks, coupled

Table 1. Elemental abundance for analyzed materials, Al values reported in %, the other elements are expressed in ppm.

			Al	K	Cr	V	Ba	Sr	Rb	Ni	Co	Cu	Ga	Mo	Th	U	Y	La
Target Rocks	C. Arenite	TR1	0.18	684	31.8	10.1	29.4	13.9	1.02	14.5	<0.001	3.88	1.42	0.79	1.05	0.32	3.76	6.08
		TR2	0.09	195	64.0	4.80	30.2	12.7	0.78	26.4	0.55	1.87	1.00	1.94	0.62	0.25	2.73	3.36
		TR3	0.07	178	18.6	4.42	45.7	86.6	3.37	10.0	0.76	25.3	1.26	1.52	0.56	0.27	11.2	14.5
		Mean	*0.11*	*352*	*38.1*	*6.44*	*35.1*	*37.7*	*1.72*	*17.0*	*0.66*	*10.4*	*1.23*	*1.42*	*0.74*	*0.28*	*5.90*	*7.98*
		S.D.	*0.06*	*287*	*23.4*	*3.18*	*9.19*	*42.3*	*1.43*	*8.47*	*0.15*	*13.0*	*0.21*	*0.58*	*0.27*	*0.04*	*4.62*	*5.81*
	Siltite	TR4	0.61	335	151	30.6	167	355	8.80	45.3	10.8	5.45	11.5	4.45	4.15	1.59	181	179
		TR5	0.81	460	173	35.2	241	583	15.4	57.3	11.1	4.77	15.3	5.13	4.64	1.94	288	311
		Mean	*0.71*	*398*	*162*	*32.9*	*204*	*469*	*12.1*	*51.3*	*11.0*	*5.11*	*13.4*	*4.79*	*4.40*	*1.77*	*235*	*245*
		S.D.	*0.14*	*88.4*	*15.6*	*3.25*	*52.3*	*161*	*4.67*	*8.49*	*0.21*	*0.48*	*2.69*	*0.48*	*0.35*	*0.25*	*75.7*	*93.3*
Fallback Deposits																		
		FB1	0.15	367	103	12.8	87.7	317	16.3	979	32.1	7.34	1.11	3.83	1.37	0.62	77.3	76.6
		FB2	0.21	398	68.5	13.7	16.0	321	13.6	544	4.42	6.20	1.58	0.79	1.66	0.8	118	119
		FB3	0.19	451	71.1	15.1	40.0	343	21.8	615	10.8	6.67	1.44	1.21	1.76	0.87	113	97.0
		FB4	0.21	559	93.8	17.0	36.2	344	25.8	1226	16.1	8.26	1.49	1.50	1.34	0.62	72.1	80.4
		FB5	0.21	653	89.0	19.1	26.0	359	31.4	1228	11.2	9.73	1.48	0.96	1.55	0.73	81.2	98.6
		FB6	0.16	831	94.9	13.1	48.0	600	27.6	606	13.4	12.5	1.15	2.75	1.32	0.62	60.0	84.6
		Mean	*0.19*	*543*	*86.7*	*15.1*	*42.3*	*381*	*22.8*	*866*	*14.7*	*8.45*	*1.38*	*1.84*	*1.5*	*0.71*	*86.9*	*92.7*
		S.D.	*0.03*	*177*	*13.88*	*2.48*	*24.87*	*109*	*6.84*	*319*	*9.38*	*2.35*	*0.20*	*1.20*	*0.18*	*0.11*	*23.3*	*15.6*
Impactite clasts	Light Glass	IC1	0.27	1810	121	179	64.3	568	65.1	1965	4.89	30.9	3.30	2.26	1.85	1.12	88.0	112
		IC2	0.17	1704	97.7	19.4	66.0	513	60.8	111.6	3.52	12.4	3.64	2.31	1.36	0.64	61.5	330
		IC3	0.03	570	83.5	12.4	136	516	16.4	881	1.02	11.3	1.68	1.89	0.14	0.28	14.6	35.2
		IC4	0.08	1261	67.8	17.9	24.7	495	43.6	97.3	25.2	7.85	2.85	1.84	0.61	0.58	42.3	97.4
		IC6	0.13	436	88.7	6.23	63.4	414	12.7	598	2.82	2.75	2.90	3.01	1.69	0.54	58.5	134
		IC7	0.18	697	68.6	9.53	89.3	744	21.1	3213	2.45	3.80	2.98	2.69	2.74	0.9	62.2	108
		IC8	0.07	861	112	21.2	199	702	31.6	127.7	2.79	11.8	3.54	2.35	0.48	0.61	33.6	157
		Mean	*0.13*	*1048*	*91.3*	*38.0*	*91.8*	*565*	*35.9*	*999*	*6.10*	*11.5*	*2.98*	*2.34*	*1.27*	*0.67*	*51.5*	*139*
		S.D.	*0.08*	*550*	*20.4*	*62.4*	*58.0*	*118*	*21.17*	*1181*	*8.50*	*9.37*	*0.65*	*0.41*	*0.91*	*0.27*	*23.7*	*92.2*
	Dark Glass	IC9	0.66	2212	402	57.22	69.6	764	81.5	23010	401	69.2	9.27	2.58	5.11	2.27	324	341
		IC10	0.57	1617	639	43.2	166	683	57.5	10550	1091	92.6	10.3	8.33	3.75	1.79	237	248
		Mean	*0.62*	*1915*	*521*	*50.2*	*118*	*724*	*69.5*	*16780*	*746*	*80.9*	*9.79*	*5.46*	*4.43*	*2.03*	*281*	*295*
		S.D.	*0.06*	*421*	*168*	*9.91*	*68.2*	*57.3*	*17.0*	*8811*	*488*	*16.55*	*0.73*	*4.07*	*0.96*	*0.34*	*61.5*	*65.8*
Aeolian Sands																		
		SB1	0.08	1028	56.4	5.91	54.4	330	40.9	<0.001	0.81	1.37	1.54	2.40	0.77	0.30	25.5	62.4
		SB1°	0.08	1095	89.7	6.03	17.3	523	43.0	34.9	0.93	0.47	1.64	4.61	0.66	0.34	24.3	71.9
		SB2	0.14	1700	55.3	11.8	61.2	409	62.8	51.6	3.47	2.43	1.77	2.44	1.69	0.68	58.2	93.1
		SB3	0.15	1580	28.8	12.7	26.9	587	53.2	46.2	3.98	1.52	2.16	2.33	1.40	0.62	52.3	92.8
		SB4	0.10	1291	74.6	7.24	58.47	370	40.2	38.4	1.34	3.39	1.98	2.72	1.18	0.48	38.8	92.9
		Mean	*0.11*	*1339*	*61.0*	*8.74*	*43.7*	*444*	*48.0*	*42.8*	*2.11*	*1.84*	*1.82*	*2.90*	*1.14*	*0.48*	*39.8*	*82.6*
		S.D.	*0.03*	*295*	*22.9*	*3.27*	*20.1*	*108*	*9.78*	*7.54*	*1.50*	*1.11*	*0.25*	*0.97*	*0.43*	*0.17*	*15.3*	*14.5*

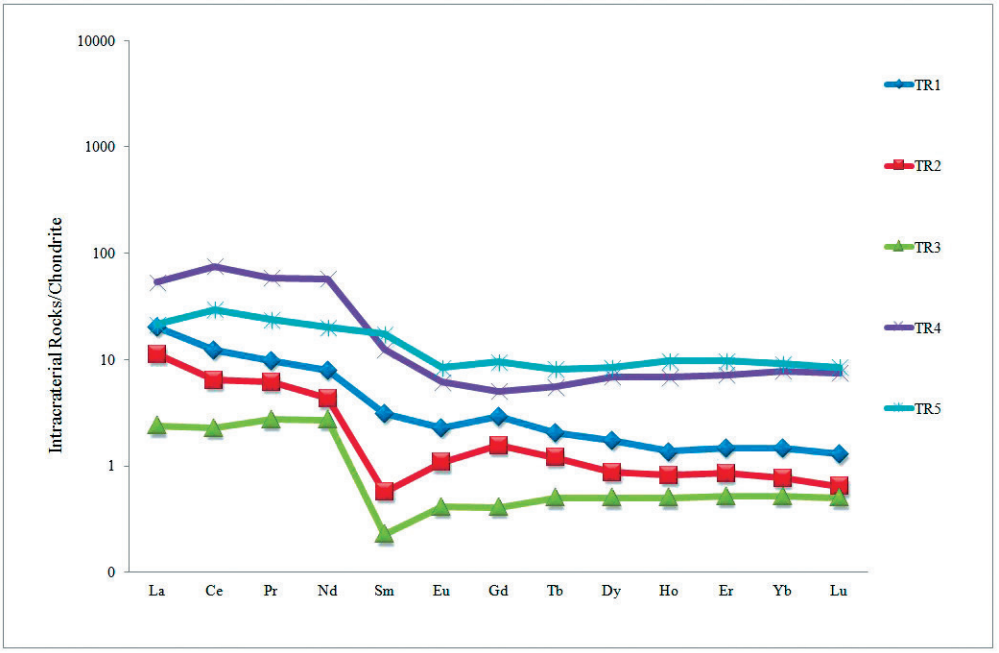

Figure 1. REE pattern for Intracraterial rocks.

Figure 2. REE pattern for Fallback deposits.

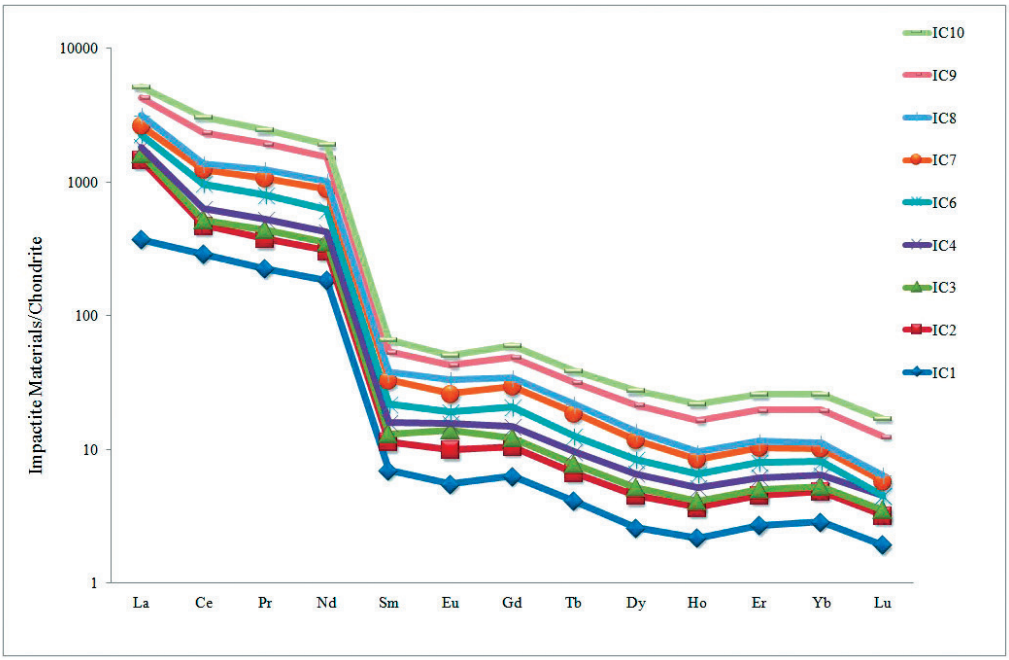

Figure 3. REE pattern for Impactite materials.

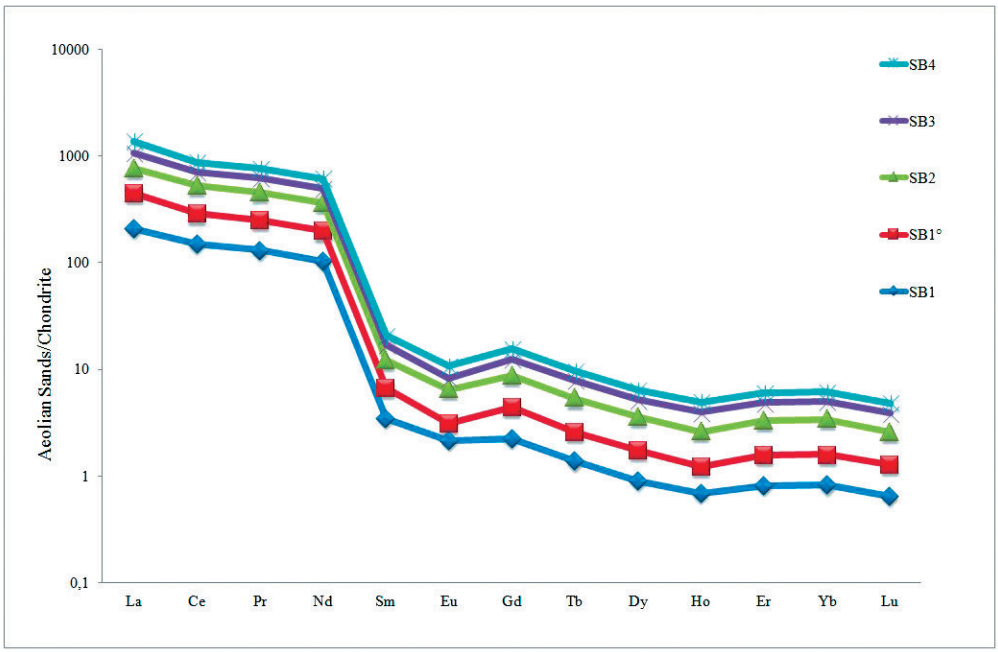

Figure 4. REE pattern for Aeolian Sands.

with petrological observations, confirm their hypersilic nature correlated to the overabundance of silica phases (essentially detrital quartz). Despite the limited number of samples analyzed, data on exposed target rocks suggest significant chemical differences between the two main rock types present (quartz arenites and the fine-grained siltistones). The latter are significantly enriched in a series of both lithophile and siderophile elements such as K, Th, REE, Cr, Ni, Co (Table 1 and Figure 1). This obviously reflects differences in their mineralogy, in particular a major abundance in siltstones of a kaolinite matrix. Lithophile element chemistry of the intracraterial fallback deposits appears intermediate between that of sandstones and siltstones (see also REE patterns in Figure 2). As fallback deposits consist of material formed by instantaneous fragmentation and pulverization of all material affected by impact, in principle its composition in terms of lithophile elements should be considered the most representative of the "average" composition of terrestrial target rocks involved in the impact. Nevertheless, this deposit is strongly enriched in siderophile elements (in particular Ni) with respect to the exposed target rocks. This obviously reflects the contamination by components of the metallic impactor. Our observations under the optical and electron microscope suggest that these components are present in fallback deposit in different forms (i.e., unmelted metal particles, melted metal drops, etc.); similar to those observed also in vitreous ejecta clasts (Folco et al., 2011; Fazio et al., 2014). The distribution of most lithophile elements (e.g., Al, K, Cr, Th, and U) in individual light-coloured impactite clasts indicates that their composition is rather heterogeneous. However, the average composition of these vitreous products is compatible, except for some elements like Sr, Ba, Y and REE, with a possible average composition of the target material based on an appropriate mixture of the two main constituents (quartz arenites and siltstones) as deduced by observation on the exposed crater rocks. All individual light-coloured vitreous clasts analyzed contain rather variable amounts of siderophile elements (Ni, Co, Cu) much above their abundance in target rocks (Table 1). Such finding obviously confirms the petrographic observations on the presence of appreciable amounts of impactor-derived components in all the impact melting products. REE patterns in most vitreous ejecta are rather similar except for slight negative Ce anomalies in some samples sometimes coupled with positive Eu anomalies (Figure 3). Usually, these anomalies are correlated to specific oxidation states of the elements which control their behaviour in both magmatic and sedimentary environments. Ce anomalies in sediments are usually correlated to the different mobility of Ce^{4+} when compared to the REE^{3+} during water/rock interaction processes (Loges et al., 2012). In particular, negative Ce anomalies characterize products of intense weathering and/or laterization processes (Braun et al., 1990). Therefore, the presence of negative Ce anomalies coupled with a positive Eu anomaly in one Kamil vitreous clast possibly suggests weathered bedrocks as a possible terrestrial source.

Information on the chemistry of dark-coloured vitreous ejecta drawn from the data on the two composite samples (IC-9 and IC-10) seem to indicate that the "average" composition of such melted ejecta differ significantly from that white glasses and of any possible mean composition of the crater excavated material. In fact, they are strongly enriched in lithophile elements (see Table 1 and Figure 3), in particular in K, Sr, Y and REE and in the siderophile elements (especially in Ni and Co). This last finding is easily explainable with a larger presence of metal-derived component as also evidenced by Fazio et al., 2014. The data indicate that dark-coloured vitreous material is enriched also in Ga and Mo, known to be concentrated in some meteoritic metals with respect to terrestrial

materials. Terrestrial processes (e.g., oxidative weathering and laterization) may concentrate these elements in residual soils; therefore the origin of their presence in vitreous products is questionable. Lithophile and siderophile element chemistry of aeolian sands is indistinguishable from that of the substratum detrital rocks. The abundance of most main and trace elements is intermediate between the elements found in sandstone and siltstone target rocks (see Table 1 and Figure 4). They show very low Ni, Co and Cu abundances also in samples collected very proximal to the impact site and this excludes any appreciable contaminations by projectile components. It is worthy of note that in the same sand samples, including also those collected at a considerable distance from the crater (more than 1.5 km), high-pressure impact mineral phases like coesite and stishovite were ubiquitously found (Sighinolfi et al., 2014).

Oxygen isotope data

The $\delta^{18}O$ values for the different materials analyzed are reported in Table 2. The available data on the intracraterial target rocks seem to suggest that the most widespread substratum quartz-arenites are isotopically very homogeneous and similar either to fallback deposits or to recent aeolian sands. The $\delta^{18}O$ values of these materials, ranging from 11.1‰ to 12.6‰, are compatible with their mineralogy consisting of detrital quartz grains (frequently quartz > 98% volume) resulting from the disaggregation of ancient granitoid rocks. Samples of fine-grained hypersilicic rocks (siltstones) interbedded with arenites are strongly enriched in ^{18}O ($\delta^{18}O$ = +16.3‰). The enrichment in ^{18}O in these fine-grained hypersilicic layers may reflect primary sedimentary features or post-depositional history of detrital quartz components. Biosiliceous sediments and opaline silica are usually characterized by strong enrichments in ^{18}O with respect to normal detrital quartz rocks (Behl and Smith, 1992). Microcrystalline recrystallized silica deposits (cherts) are known to be frequently enriched in ^{18}O (Knauth and Epstein, 1976; Knauth and Lowe, 1978). In general, during the diagenesis of silicoclastic sediments, the secondary precipitated silica phases (cement) were significantly enriched in ^{18}O (Harwood et al., 2013; Lyon et al., 2009). Observations under the optical microscope indicate that the Kamil target siltstone, largely made up of a fine matrix of secondary quartz crystals, shows strong affinities with chert deposits; therefore, the enrichment in ^{18}O could reflect a secondary silicification process. Fallback deposits show a relatively constant oxygen isotope chemistry and result slightly enriched in ^{18}O with respect to the most common target rocks (Table 2), i.e. quartz arenites. Their $\delta^{18}O$ values are consistent with a model of target source material which includes the predominance of quartz arenites and only minor amounts of siltstones. As previously observed, in consideration of their source processes, fallback deposits should be considered representative of the "average" chemical and isotopic composition of the whole substratum rocks, which were disaggregated and pulverized during the impact. Possibly, their oxygen isotope chemistry represents also a regional signature for the whole bedrock and perhaps it is not a coincidence that the $\delta^{18}O$ values of fallback deposits overlap those of aeolian sands (see Table 2). Oxygen isotope data on impact melt products show a relative heterogeneity ($\delta^{18}O$: 13.1 to 14.3‰) with a significant enrichment in ^{18}O with respect to both the main diffused substratum rocks (quartz arenites) and the presumed "average" composition of the excavated material deduced from the data on fallback deposits. In particular, dark-coloured vitreous ejecta result significantly enriched in ^{18}O also with respect to white glasses. As the $\delta^{18}O$ values of vitreous clasts result intermediate between those of target quartz arenites and siltstones, their variations would simply reflect different mixtures of the two main target rocks in the source material.

Table 2. $\delta^{18}O$ values for diffeent materials analyzed.

	Material	$\delta^{18}O$‰ V SMOW	$\delta^{18}O$ ‰ SMOW (*mean value*)
Target Rocks			
TR-1	Coarse grained target arenite	11.4 - 11.4	11.4
TR-2	Coarse grained target arenite	11.8 - 11.6	11.7
TR-3	Coarse grained target arenite	11.1 - 11.1	11.1
TR-4	Fine-grained siltstone	16.2 - 16.4	16.3
TR-5	Fine-grained siltstone	16.2 - 16.4	16.3
Fallback Deposits			
FB-1	Fine grained pulverized target rocks	11.9 - 12.1	12.0
FB-2	Fine grained pulverized target rocks	12.2 - 12.2	12.2
FB-3	Fine grained pulverized target rocks	12.2 - 12.6	12.4
FB-4	Fine grained pulverized target rocks	11.7 - 11.7	11.7
Impactite Clasts			
IC-1	Light-coloured clast	13.0 - 13.2	13.1
IC-2	Light-coloured clast	13.9 - 13.9	13.9
IC-3	Light-coloured clast	14.2 - 14.2	14.2
IC-9	Dark-coloured clast	14.2 - 14.5	14.3
IC-10	Dark-coloured clast	14.4 - 14.4	14.4
KQz1	Quartz separeted from IC1 sample	10.8 - 10.8	10.8
Aeolian Sands			
SB-1	<500 µm fraction	11.5 - 11.5	11.5
SB-3	<500 µm fraction	12.2 - 12.2	12.2

However, the rate of enrichment in ^{18}O results, especially in dark glasses, results poorly compatible with any possible mixture of the two rock types taking into account the relative scarcity of siltstones layers within the crater exposed rocks. The analysis of residual quartz grains separated under the optical microscope from a light-coloured vitreous clasts (sample IC-3, see Table 3), reveals a $\delta^{18}O$ value (10.8‰) typical of detrital quartz and significantly lower than the value (13.9‰) of the bulk vitreous clasts. Once discarded, on the basis of physical grounds, the hypothesis that the transient impact melting of terrestrial material may introduce significant isotope fractionation the oxygen isotope chemistry of the Kamil impact glasses requires a terrestrial source different from that represented by the exposed target rocks.

Discussion

The role of the impactor on melting processes and element fractionation during explosive impact

The distribution of siderophile elements in materials presents in the Kamil area and in particular in vitreous ejecta clasts and fallback deposits may shed light on the direct involvement of the impactor in the melting

processes of terrestrial materials and on possible element fractionations which were active during the explosive disruption of the impacting body. The composition of the impactite ejecta, i.e., the abundance levels of siderophile elements, indicates that melting of terrestrial material occurred exclusively when components of the impactor were directly involved in melting. In addition, the overabundance of the mass of dark glasses enriched in projectile-derived elements with respects to white glasses indicates that the rate of melting of terrestrial materials is controlled by the amount of projectile components involved in melting. Such a close association of terrestrial materials with projectile components in the Kamil impactites suggests that vitreous ejecta may have formed by a dense, hot spray of partially melted projectile and target materials. This scenario is consistent both with the distribution of microscopic impact debris in soils in the Kamil area and with the fact that impactor components in melted impactites are present in various forms (i.e., as unmelted metal particles and fragments, melted metal drops etc.). A comparative analysis of chemical and isotopic data indicates that the mass and composition of the products of impact melting depend also on the nature and localization of terrestrial materials involved in melting. The relatively small mass of white vitreous ejecta chemically and isotopically compatible with the exposed intracrateric target rocks suggests that these rocks were only minimally affected by impact melting. In addition, the data suggest that melting of such rocks occurred in presence of a reduced component of the projectile. Most of the mass of the Kamil glasses, i.e. the dark vitreous impactites, requires an alternative source material. A discussion of possible terrestrial sources for these impactites will be given in the next paragraph. The comparison between the initial composition of materials (both of terrestrial and projectile origin) involved in hypervelocity impacts and that of products of heating and melting may provide information on element fractionation during the process. In the present case the discussion may include only some siderophile elements (Ni, Co and Cu) whose abundance levels in the projectile are well known and which in the Kamil rocks are present at very low concentrations. Therefore, comparison of the Ni-Co-Cu ratios in the Kamil terrestrial formations contaminated by projectile components may be useful to test whether element fractionation occurred. Other siderophile elements like iron cannot be considered as their origin in both impactites and fallback deposits may be questionable (i.e., terrestrial or correlated to the impactor). Analysis of different fragments of the Kamil projectile (Urbini et al., 2012) indicates a very homogeneous composition especially in term of abundance of Ni, Co and Cu. Table 3 reports ranges and average values for the Ni-Co and Ni-Cu ratios in the impactor, in fallback deposits and light- and dark-coloured vitreous ejecta. The Ni-Cu and Ni-Co relationships are reported in graphical form on Figures 5 and 6, respectively. The data show that ratios in fallback deposits and impactites are extremely variable and significantly different from those of the projectile. In these materials the projectile component is significantly enriched in Ni with respect to Co. These data seem to agree with the results of SEM-EDX analysis of Fe-Ni spherules in impactite clasts (D'Orazio et al., 2011), indicating a general Ni enrichment with respect to the bulk metals of the Gebel Kamil iron. Contrasting indications result from the Ni-Cu abundance ratios, with Cu resulting more concentrated with respect to Ni in fallback deposits and in most vitreous white and dark clasts but not in the IC-10 sample. The latter is a composite sample representative of dark-coloured vitreous clasts of major mass collected in the proximity of the crater. It should be noted that the present data cannot provide information on the mechanism of element fractionation.

Table 3. Ratio Ni/Co and Ni/Cu for materials analyzed.

	Ni/Co	Ni/Cu
Kamil Metorite (D'orazio et al., 2011)		
Shrapnel	27	472
Individual body (83Kg)	27	491
Fallback Deposits (6 samples)		
Min.	31	49
Max.	1234	148
Mean	64	106
Light impactite clast (7samples)		
Min.	4	9
Max.	1311	845
Mean	423	176
Dark impactite clast (composite samples)		
IC-9	57	332
IC-10	191	1932

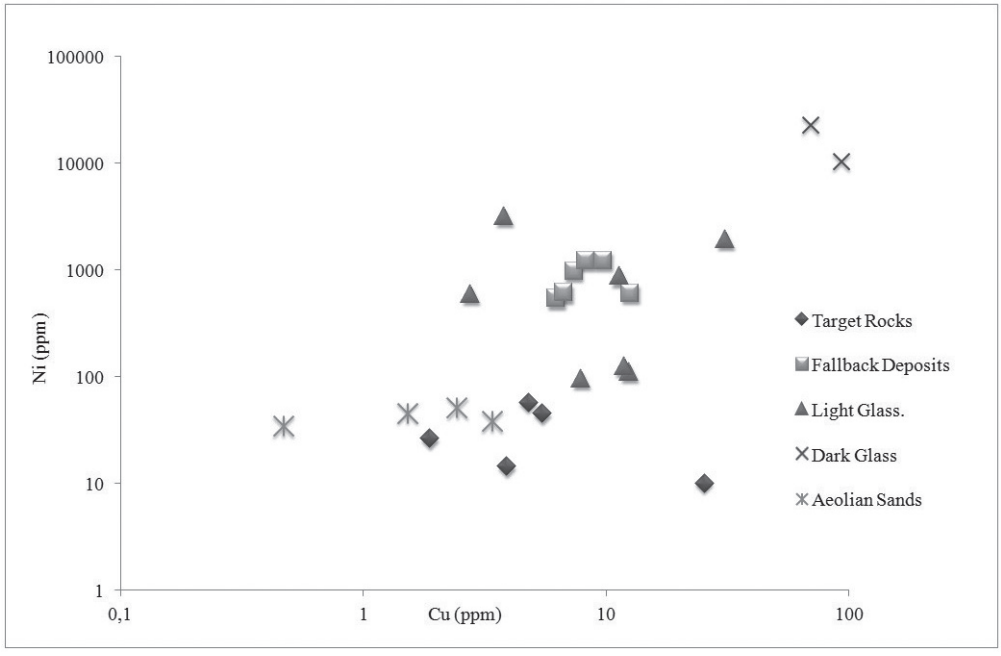

Figure 5. Ni/Cu relationship for samples analyzed.

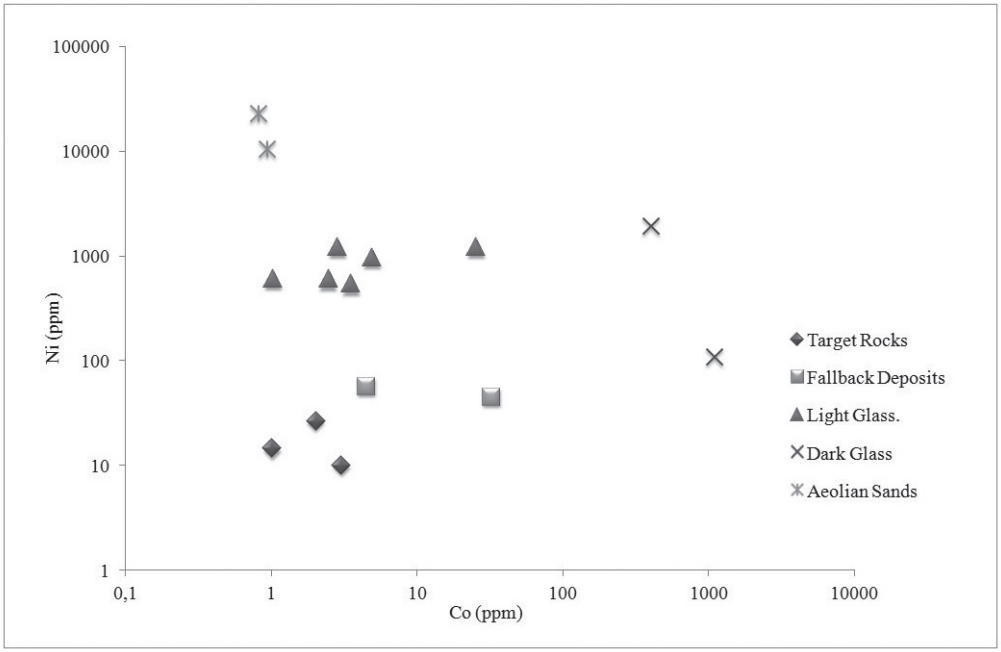

Figure 6. Ni/Co relationship for samples analyzed.

They refer to the bulk composition of the projectile component are present in impact glasses and fallback deposits and we know that it is present under different forms (i.e. melted and unmelted metal particles vapour condensates and dissolved in silica-rich melts) as consequence of different forming processes.

Possible terrestrial sources for impactite ejecta products

Comparative analysis of chemical and isotope data on intracrateric target rocks and on products of impact melting and considerations on the relative mass abundance of white and dark coloured vitreous ejecta allow some hypotheses regarding their terrestrial source materials. It has been shown that lithophile element abundances in white impactite clasts, which make up only a minor component of the entire mass of melted products, suggests that a mixture of the two main represented target rock types (quartz arenites and siltstones) may be the most likely source. Also oxygen isotope data support this hypothesis since their enrichment in ^{18}O with respect to more common rock types (quartz arenites) indicates a greater involvement of siltite components in melting processes than it should be expected. Much more problematic is the attribution of a terrestrial source for dark-coloured vitreous ejecta clasts which make up almost the total mass of melted materials. As reported before, for these products the only chemical and isotope information available were provided not by the analysis of individual ejecta but only by data on two composite samples representative of two classes of clasts, distinct on the basis of clast mass and localization with respect to the impact site. Since for smaller clasts the data were obtained by considering a relative large number (20) of individual clasts, they should be considered representative of a possible "average" composition of them,

whereas the same cannot be said for impactite clasts of major masses. Since no appreciable differences in lithophile elements and oxygen isotope chemistry exist between the two types of impactites, a unique terrestrial source should be determined for all dark-coloured melted materials. It has been shown that chemical and isotope signatures of dark glasses are not compatible with a source represented by any possible "average" composition of the target material deduced by observations on exposed target rocks. On the other hand, similar signatures may be attained only if we admit that a target siltstones component has been selectively involved in melting with respect to the arenite component. Theorically, this scenario may have occurred as observation on the exposed crater rocks indicted that the rock types are not homogeneously distributed within the sequence of substratum rock (Urbini et al., 2012). We retain, however, that the preferential involvement of fine grained siltstone in impact melting is unable to explain the chemical and isotope features of dark vitreous ejecta. In the present paper we focused our attention almost exclusively on target rocks exposed on the crater walls, although other terrestrial materials may have been involved in the impact event. Reconstruction of the pre-impact surface stratigraphy based on field geological observations and supported also by data of seismic profiles (Urbini et al., 2012) in areas proximal to the crater points to the presence of an approximately 2 m thick surface layer, characterized by low P-wave which can be ascribed to an unconsolidated, dry top cover superimposed on the sequence of consolidated rocks. Urbini et al. (2012) estimate the total volume of the excavated mass of terrestrial material in the order of 3800 m^3. Considering the calculated thickness of the unconsolidated cover, the excavated mass of terrestrial material should include a minimum 1200 m^3 of this cover. We have no information about the origin and mineralogical, chemical and isotope signatures of this unconsolidated cover. Theoretically, such cover could be constituted by transported materials (fluvial, aeolian) or by loose deposits formed in situ during alteration of substrate rocks. Considering main features of the regional surface geology and the thickness of the cover, we suggest that the most likely formation process is alteration-weathering active under paleoclimate conditions quite different from recent or present day climate conditions. According to this hypothesis we can argue about the changes that weathering may have introduced in the mineralogy and chemical and isotope features of the consolidated substrate rocks. The changes would be correlated to the dissolution of primary phases (essentially detrital quartz grains and albite) and to formation of new stable phases under surface conditions. They may include secondary silica phases, clay minerals (essentially kaolinite), Fe-hydroxides and other phases precipitating under oxidative conditions (phosphates, etc.). Thus, it should be expected that the weathered surface cover became enriched in a series of elements (Al, Fe, K, REE, etc.) enclosed in these secondary phases with respect to the unaltered substrate bedrock. Weathering and/or laterization processes may also introduce anomalies in the REE patterns (Braun et al., 1990; Loges et al., 2012) similar to negative Ce anomalies and positive Eu anomalies shown by some samples of the Kamil vitreous ejecta. On the basin of such assumptions relative to the possible chemical features of the pre-impact unconsolidated cover we retain that this may represent the most suitable source for most kamil vitreous materials, in particular for dark-coloured impactite ejecta glasses. If this is true, we can conclude that in the case of small-scale hypervelocity impact such as the Kamil event, appreciable melting of terrestrial material occur only at or very nearly to the earth's surface and with the direct involvement of projectile constituents.

Acknowledgements

The authors are grateful to Prof. Antonio Longinelli, University of Parma, for the oxygen isotope analysis; Two anonymous reviewers helped to substantially improve this manuscript as did the comments of editorial assistant Michele Lustrino.

References

Behl R.J. and Smith B.M. (1992) - Silicification of deep-sea sediments and the oxygen isotope composition of the diagenetic siliceous rocks from the Western Pacific Pigafetta and East Mariana Basins, LEG 129. In: Larson, R.L., Lancelot Y. ,et al. (Eds) Proceeding of the Ocean Drilling Program, Scientific Results, College Station, Tx, 129, 81-117.

Braun J.J. (1990) - Cerium anomalies in lateritic profiles. *Geochimica et Cosmochimica Acta*, 54, 781-795.

D'Orazio M., Folco L., Zedoli A. and Cordier C. (2011) - Gebel Kamil: The iron meteorite that formed the Kamil crater (Egypt). *Meteoritics & Planetary Science*, 46, 1179-1196.

Fazio A., Folco L., D'Orazio M., Frezzotti M.L., and Cordier C. (2014) - Shock metamorphism and impact melting in small impact craters on Earth: evidence from kamil crater, Egypt. *Meteoritics & Planetary Science,* 49, 2175-2200.

Folco L., Di Martino M., El Barkooky A., D'Orazio M., Lethy A., Urbini S., Nicolosi I., Hafez M., Cordier C., van Ginneken M., Zeoli A., Radwan A.M., El Khrepy S., El Gabry M., Gomaa M., Barakat A.A., Serra R. and El Sarkawi M (2010) - The Kamil crater in Egypt. *Science*, 329, 804.

Folco L., Di Martino M., El Barkooky A., D'Orazio M., Lethy A., Urbini S., Nicolosi I., Hafez M., Cordier C., Van Ginneken M., Zeoli A., Radwan A.M., El Khrepy S., El Gabry M., Gomaa M., Barakat A.A., Serra R. and El Sarkawi M. (2011) - Kamil Crater (Egypt): ground truth for small-scale meteorite impacts on Earth. *Geology*, 39, 179-182.

Folco L., Fazio A., Cordier C., van Ginneken M. and D'Orazio M. (2012) - Microscopic impactor debris in the soil around Kamil crater (Egypt): implications for impact scenario. *Meteoritics & Planetary Science* Supplement, (abstract 5198).

Folco L., Fazio A., D'Orazio M., Cordier C., Zeoli A., van Ginneken M. and El-Barkooky A. (2013) - Nickel concentration in the soil around Kamil crater (Egypt). *Meteoritic & Planetary Science* Supplement (abstract 5295).

Harwood J., Aplin A.C., Fialips C.I., Iliffe E., Kozdon R., Ushikubo T. and ValleY J. (2013) - Quartz cementation hystory of sandstones revealed by high-resolution SIMS oxygen isotope analysis. *Journal of Sedimentary Research*, 83, 522-530.

Klizsch E., Harms J.C., Lejal-Nicol A. and List F.K.(1979) - Major sudvisions and depositional environments of the Nubia strata, south-western Egypt. *American Association of Petroleum Geologists Bulletin*, 63, 967-974.

Knauth L.P. and Epstein S. (1976) - Hydrogen and oxygen isotope ratios in nodular and bedded cherts. *Geochimica et Cosmochimica Acta*, 40, 1095-1108.

Knauth L.P. and Lowe D.R. (1978) - Oxygen isotope geochemistry of cherts from the Onderwacht Group (3.4 billion years), Transvaal, South Africa, with implications for secular variations in the isotopic composition of cherts. *Earth Planetary Science Letters*, 41, 209-222.

Loges A., Wagner T., Matthias B., Bau M., Gob S. and Markl G. (2012) - Negative Ce anomalies in Mn oxides: The role of Ce^{4+} mobility during water-mineral interaction. *Geochimica et Cosmichica Acta*, 86, 296-317.

Longinelli A., Sighinolfi G., De Michele V., Selmo E. (2011) - δ18O and chemical composition of Libyan Desert Glass, country rocks, and sands: New considerations on target material. *Meteorics and Planetary Science,* 46, 218-227.

Lyon I.C., Burley S.D., McKeever P.J., Saxton J.M. and Macaulay C. (2009) - Oxygen isotope analysis of authigenic quartz in sandstones: a comparison of ion microprobe and conventional analytical techniques. In: Quartz cementation in sandstones (Eds R.H. Worden and S. Morad). Blackwell Publishing Ltd., Oxford, UK, doi: 10.1002/9781444304237.ch20.

McDonough W.F. and Sun S. (1995) - The composition of the Earth. *Chemical Geology,* 120, 223-253.

Melosh H.J. (2013) - The contact and compression stage of impact cratering. In: *Impact cratering*, edited by Osinki G.R. And Pierazzo E. Chichester, West Sussex, UK: Wiley-Blackwell. pp. 32-42.

Sighinolfi G.P., Elmi C., Serra R. and Contini G. (2014) - High density silica phases as evidence of small-scale hypervelocity impacts: the Gebel Kamil crater (Egypt). *Periodico di Mineralogia,* 83, 299-312.

Sighinolfi G.P., Martini M., Sibilia E. and Contini G. (2015) - Thermoluminescence dating of the Kamil impact crater (Egypt). *Meteorics and Planetary Science,* 50, 204-213.

Urbini S., Nicolosi I., Zeoli A., El Khrepy S., Lethy A. and Hafez M. (2012) - Geological and geophysical investigation of Kamil crater, Egypt. *Meteoritics & Planetary Science*, 47, 1842-1868.

Submitted, December 2014 - Accepted, April 2015